International Journal of Advanced Educational Research
ISSN: 2455-6157
Impact Factor: RJIF 5.12
www.educationjournal.org
Volume 3; Issue 1; January 2018; Page No. 383-389

Structural and gas sensing properties of nanocrystalline WO_3:TiO_2-based hydrogen gas sensors

Anoop Kumar
M.Sc. Chemistry, CH. Dadri, Haryana, India

Abstract
This paper deals with the study of nanocrystalline TiO_2:WO_3-based hydrogen sensors. Using conventional techniques like XRD, SEM and TG-DTA performed structural characteristics. XRD of undoped TiO_2 calcined at 600°C for 6 h shows good crystalline quality having a 54 nm grain size. The sensitivity was improved by adding 15 wt% WO_3.TiO_2 based H_2 gas sensor. The operating temperatures of the sensors were optimized under different operating conditions. TiO_2 sensor doped with 15-wt % WO_3 and 0.5 wt % Pt showed the maximum response to H_2 with a higher selectivity at an operating temperature of 200°C. The electronic interaction between the additive and the oxide semiconductor is proposed to account for the sensitization effects.

Keywords: nanocrystalline, XRD, SEM, TG-DTA

Introduction

The growing demand of fast, accurate and low cost air quality analysis techniques for domestic and industrial environmental monitoring, automotive applications, air conditioning and sensors networks is tailoring the research toward new materials and techniques to solve the problems related to the commercial sensors. Metal-oxide semiconducting layers are the most promising conductometric chemical sensors among solid-state devices, due to their low dimension, price and power consumption [1-12].

The sensing properties are based on reactions between semiconductor oxides and gases in the atmosphere. These reactions produce changes in electrical properties of semiconductors. There are many possible reactions; the most common reaction that leads to changes in conductivity is the adsorption of gases on the semiconductor surface. It is known that the resistance of semiconducting films is strongly influenced by the presence of oxidizing or reducing gases [13]. Oxygen in the atmosphere can be adsorbed on the semiconductor surface in different species (O_2, O^{2-} and O"). The charge exchange between the adsorbed molecules and the semiconductor oxide layers modifies the energy barrier eV_s for grain-to-grain current percolation and in turn the electrical conductance of the layers. Accordingly, the conductance of the layer can be expressed by: -

$$G = G_O \exp(-eV_s / kT) \quad \text{-------(1)}$$

Where G_O is a constant. The interaction of an oxidizing (reducing) gas occurs with either the film surface or the oxygen adsorbates. It results in donating (capturing) electrons at the semiconductor surface, which leads to a positive (negative) conductance variation for an n-type semiconductor. The opposite behavior occurs for a p-type semiconductor. In both cases, the variation in conductance, AG, depends on gas concentration [gas], according to the empirical formula [14].

$$I\Delta GI/G = A[gas]^B \quad \text{------ (2)}$$

Where A and B are constants determined by temperature, grain size, film porosity and specifically gas adsorption. The effects of the microstructure, are well recognized, including the ratio of surface area to volume, grain size and pore size of the metal oxide particles as well as film thickness of the sensor. Lack of long-term stability and selectivity has until today prevented a widespread diffusion of this type of sensors. The majority of the works done on the gas sensitive nanocrystalline semiconductor oxides aim at improving the functional parameters: sensitivity, selectivity, and response rate. Although a large number of different oxides have been investigated for their gas sensing properties, commercially available gas sensors are mainly made of $SnCO_2$ in the form of thick or thin films [15]. The effort to achieve a mixed metal oxide layer arises from the need of a stable and nanostructured material. There are many effects that can derive from these mixed systems; for example, the sensing material can be stabilized, its nanosized character can be mentioned, the presence of a second phase can maintain the grain sizes and the thickness of interface layers within dimensions comparable to the Debye length, one of the two phases could act as a filter and the other as a sensing material, and so on.

Titanium dioxide is extensively used for applications in the field of optics [16], electrical insulation [17], photovoltaic solar cells [18], electro chromic displays [19] and high-performing anodes in ion batteries [20]. Besides the "bulk" properties, titania has also been recently appreciated for production of antibacterial coatings and photo catalytic reactors [21].

Recently Liu *et al.* [22] have succeeded in preparing TiO_2 thin films by employing a sol-gel method. It is shown that the addition of a metallic phase or metal oxides to the semiconductor often improves the sensitivity and selectivity to gases. Atashbar *et al.* [23] have prepared thin films of TiO_2 by using a sol-gel method and subsequently doped with niobium oxide for use as an oxygen sensor.

Semiconducting oxide gas sensors have been used to warn of explosive gases since the1960s, but more recently other

applications in which semi conducting oxide may be Employed as sensor mate-rials have been considered, including detection of air pollutants and improving fuel efficiency in industrial combustion processes. The reducing gas depletes the coverage of adsorbed oxygen ions on the sensor surface and supplies electrons to the conduction band, leading to a fall in resistance [24]. A current goal in sensor research is to improve the sensor selectivity by eliminating similar responses from interfering gases. It has been found that the sensor selectivity and sensitivity may be altered by the addition of second oxide phases and elemental metals [25]. One such study has shown the effects of a second insulating phase on the sensing properties of anatase ($TiCO_2$). Although $TiCO_2$ is a well-known oxygen sensor [26, 27] it has more recently been used to detect and measure both CO and H_2 [28, 29]. These gases are the main con-stituents of producer gas, a reactant gas in a number of industrial processes, and are also by-products of inefficient hydrocarbon combustion; their detection is, therefore, important both in order to warn of potentially explosive gas leaks and to indicate the efficiency of combustion.

Experimental details

Fig.1 shows the flow chart for synthesis of TiO_2 nanopowder by sol- precipitation method. The precursors of TiO_2 and TiO_2 / WO_3 nanocrystallites were prepared by a sol-precipitation method, in considering the reactive conditions such as the concentration of reactants, the addition of a surfactant, the amount of WO_3 addition, pH value, reaction temperature, and time. A mixed solution of $TiCI_4$ and an appropriate amount of WCI_6 with the surfactant was, hydrolyzed by adding ammonium hydroxide drop wise to form the sol of Ti $(OH)_4$ and $W(OH)_6$ at pH 7. The sol was centrifuged and washed, and then dried at 120°C for 6 h to prepare the precursors of TiO_2 and TiO_2: WO_3 nanocrystalline composites. The dried powder then calcined at different temperatures from 400°C to 800°C in order to remove any impurities, which otherwise would react with the electrode materials of the sensor element at the final stage of sensor fabrication. For the addition of platinum as sensitizer, hydrogen hexacloroplatinate was used as a starting material. The additive WO_3 was mixed to the base material TiO_2 in different weight percentages. The calcined oxide materials were mixed with 2% polyvinylalcohol (PVA) as a binder to make a paste.

The homogeneity of the compound was confirmed by X-ray diffraction using SIEMEN D.5000 with a copper target (K_α radiation □=0.15406 nm). The morphology of the obtained powder was characterized by scanning electron microscopy (Philips, model SEM 525M). The TG and DTA analysis were carried out to study thermal properties in the temperature range of 600-1000°C range, with a heating rate of 10° C/ min in dynamic air.

In order to calculate the sensitivity, the electrical resistance of a sensor was measured in the presence and absence of H_2 at a concentration of 5000 ppm in dry air. The detail sensising calculations is given in chapter 2B. The material TiO_2: 15 wt % WO_3:0.5 wt % Pt was found to be the optimum composition for the maximum sensitivity and selectivity at an operating temperature 200°C. The cross sensitivity of the sensor was also studied to other gases, including CO, LPG and H_2S.

Sensor fabrication

The calcined oxide materials were mixed with 2 % polyvinylalcohol (PVA) as a binder to make a paste.For the gas sensing measurements the paste was coated with 2-3□ hickness on alumina tube substrates on which platinum wire electrodes were already provided for electrical contacts The electrical resistance of the element in dry air is measured by means of conventional bridge circuitery in which the element is connected to an external resistor at a circuit voltage of 10 V to calculate the electrical resistance of the element.

Results and Discussion

Structural Characterization of Nanosized Tio_2

1. Xrd Pattern of Undoped and Doped Tio_2

Fig. 2 (a) shows the XRD pattern of TiO_2 calcined at 600°C for 6 h. The prominent peaks of d = 0.353, 0.2431, 0.2378 and 0.1699 nm and corresponding crystal planes (101), (103), (004) and (105) of anatase respectively indicating good crystallinity of the TiO_2 of anatase phase Fig. 2 (b) shows that the 15 wt% WO_3 doped TiO_2, calcined at 600°C for 6 h, has also a high degree of crystallinity and complete phase formation. No extra peaks are observed due to addition of 15-wt% WO_3.The crystalline sizes, calculated according to the Scherrer equation [30], was found to be in the range of 40 - 60 nm, depending on the calcinations temperature. The TiO_2 samples were calcined with different temperature ranging from 400 to 800C, but phase transitions to rutile was not observed within our experimental accuracy. The TiO_2/WO_3 samples were calcined at 600°C showed smaller grain size than sample calcined at 400°C and 800C indicating that the driving force for the grain growth is reduced by the addition of WO_3.

2. Scanning Electron Microscopy (Sem)

Fig.3. (a&b) shows SEM of undoped TiO_2 and WO_3 doped TiO_2 calcined at 600°C. of. SEM observations shows homogeneous nanosized particles without agglomerates. The homogeneous nanosized particles are of 40 to 60 nm particle size. The samples calcined at 600°C are highly porous. A comparison of the micrographs Fig. 3 a & b shows that WO_3 doped TiO_2 calcined at 600°C maintain approximately the same particle sizes.

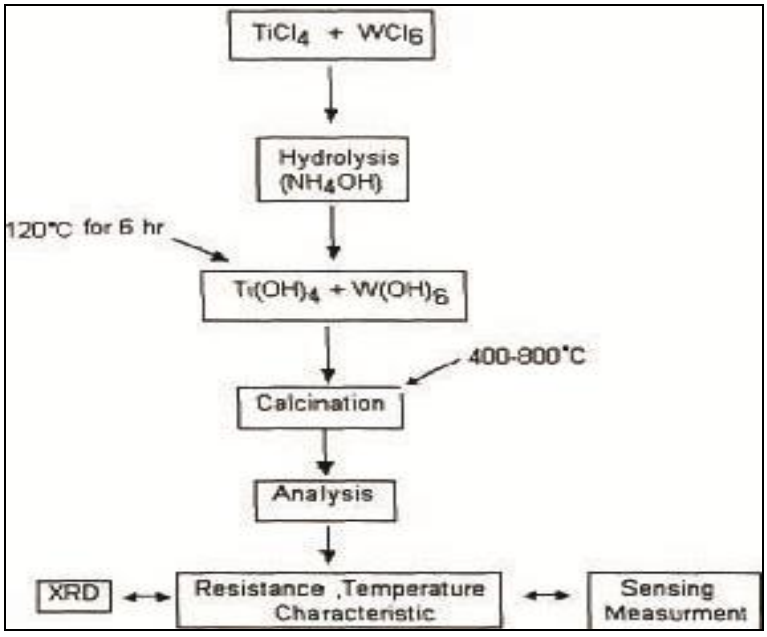

Fig 1: Flow chart for synthesis of TiO_2 nanopowder by sol-precipitation method

Dt/ Tga of Chemically Prepared Tio_2

The decomposition of compound has been checked using the differential thermal nalysis (DTA) and thermo-gravimetric analysis (TGA) shown in Fig. 4a & b. TGA curve hows peak appears at 300°C attribute to the crystallization of TiO_2.There is no weight loss above 500°C as rapid weight loss starts around 200°C.The first endothermic peak observed around 300°C shown in Fig.4b

Gas Sensing Characteristics

TiO_2 derived from sol-precipitation process requires considerably less equipment, resulting in generally lower processing costs. A major advantage of sol-precipitation methods is the ability to control the microstructure of the deposited film, *i.e.* the pore size, pore volume and surface area. The possibility to control the porosity of films is of particular interest for gas sensor application since the number of gas molecules that interact with the semiconductor surface increases with films surface area. The peculiarity of this technique to maintain good surface properties at high temperatures is also important since the response towards gases usually implies higher working temperatures.

Gas Sensing Characteristics of Commercially Available Tio_2

Commercially availableTiO_2 calcined under different calcinations temperatures. The gas sensitivity measurements shows selectivity only towards H_2 among different test gases such as H_2S, LPG and CO.Fig. 5 shows the sensitivity of commercially availableTiO_2 as a function of calcinations temperature for H_2 gas.lt was observed that sensitivity increases with increase in calcinations temperature. The sensitivity was higher 0.2 for commercially available $TiCO_2$ calcined at 700°C.

Gas Sensing Characteristics of Chemically Prepared $Ti0_2$

TiO_2 synthesized by sol-precipitation process calcined under different calcinations temperature. Fig. 6 sensitivity curve as a function of calcinations temperature shows that sensitivity increases from 0.2 to 0.5 with increase in calcinations temperature up to 600°C for H_2 gas at an operating temperature of 300°C No dominant changes observed at higher calcinations temperature. Hence the TiO_2 prepared by sol precipitation method calcined at 600°C was used for further studies.

Fig. 7. shows the sensitivity versus operating temperature for undoped TiO2 calcined at 600°C for H_2, H_2S, LPG and CO sensors. The gas sensing characteristics shows The sensitivities for H_2, LPG and CO gas are found to be 0.50, 0.43 and 0.38 at an operating temperature of 275°C, and for the H_2S gas, sensitivity observed at 0.29 at an operating temperature of 300°C.

Enhancement of Sensing Characteristics Tio_2

Development of new sensing materials should also include investigation of the structural parameters that are important for gas sensitivity and selectivity. In metal-oxide semiconducting films featuring high porosity, the electrical conductivity is determined by defects in the lattice structure, presence of dopants.

Howerver the gas sensitivity of the undoped TiO_2 was markedly promoted by the addition of several basic oxides, among which WO_3 was the most influential for hydrogen detection. The WO_3 powder prepared by a sol precipitation method was mixed in $TiCO_2$ in different amounts 5, 10, 15 and 20-wt%. From Fig.8 it was observed that the $TiCO_2$ doped with 15-wt% WO_3 shows sensitivity 0.78 for H_2.Whereas sensor doped with 5, 10 and 20-wt% WO_3 showed poorer H_2 sensing characteristics.

Fig. 9 shows the sensitivity to the four different gases for TiO_2 : 15-wt% WO_3 sensor calcined at 600°C as a function of operating temperature.,The TiO_2:15 wt% WO_3 sensor shows improvement in sensitivity for H_2, while the sensitivity was almost negligible for the other gases in the temperature range

studied. It is observed that adding WO_3, which was attributed to an increase in electrons, notably decreased the resistance of TiO_2 thick films concentration caused by W^{6+} ions substituting for Ti^{4+} ions. The defect reaction is represented as follows:-

$$WO_3 \longrightarrow W_{Ti} + O^x_o + \tfrac{1}{2}\ O_{2(g)} + 2e^- \qquad (3)$$

When operating temperature was increased from 175°C, the sensitivity for H_2 gas slowly increased to reach a maximum at 300°C as shown in Fig.9. The intrinsic conductance of a semiconducting oxide increases with increasing temperature, whereas the adsorbed oxygen on the surface gradually transforms into oxygen ions (0^-, O^{2-}) by extracting free electrons from the oxides, and thereby the conductance decreases with an increase in temperature. At a low temperature, the increase in intrinsic conductance by thermal activation

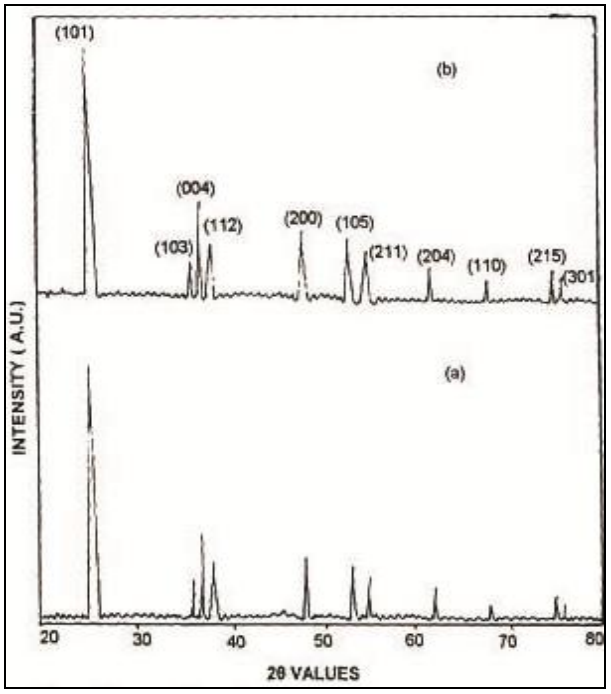

Fig 2: X-ray diffraction of (a. Undoped TiO_2b) 15 wt% $W0_3$ doped TiO_2 calcined at 600°C

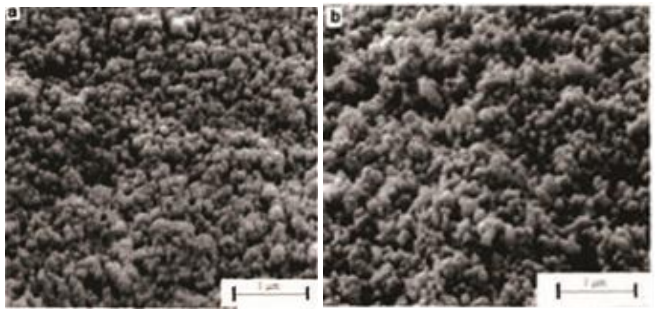

Fig 3: SEM micrographs of undoped Titania samples caldinied at (a) 600" C (b) WO_3 doped TiO_2 calcined at 600° C for 6 h

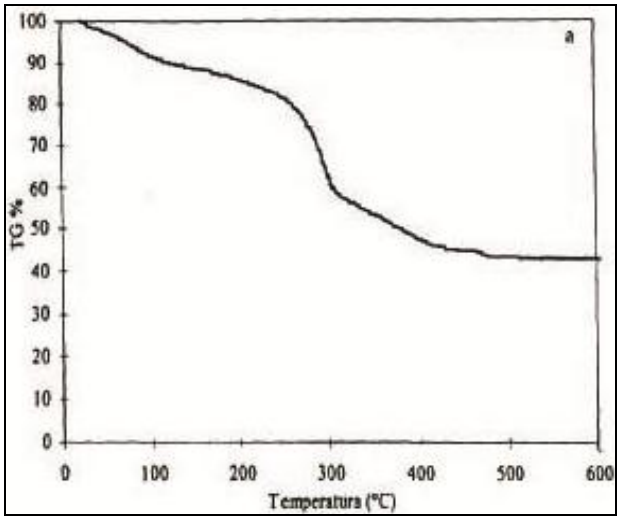

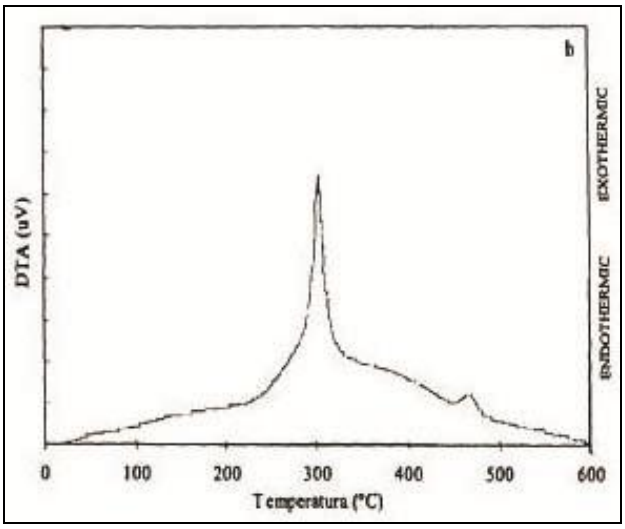

Fig 4: (a) TG and (b) DTA traces of pure Titania, recorded at a heating rate of 10°C/min.

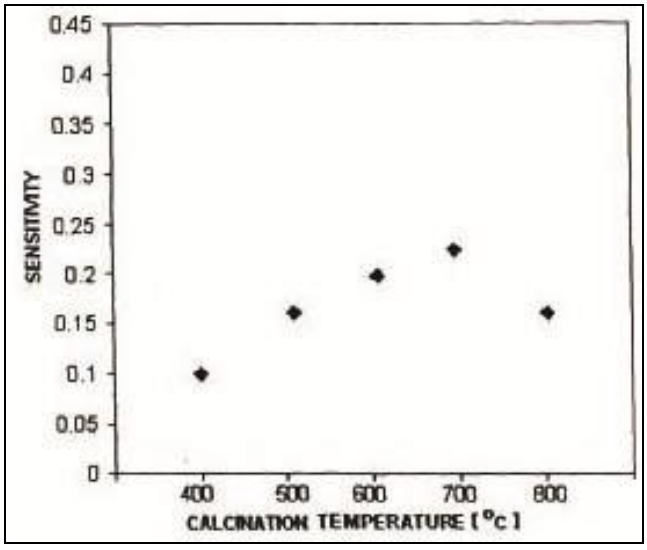

Fig 5: Sensitivity of commercially available TiO_2 as a function of calcinations temperature for H_2 gas sensor

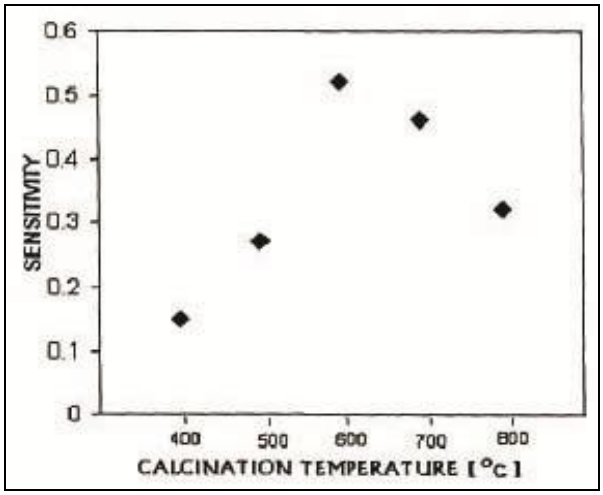

Fig 6: Sensitivity of chemically prepared TiO_2 as a function of calcinations temperature for H_2 gas sensor

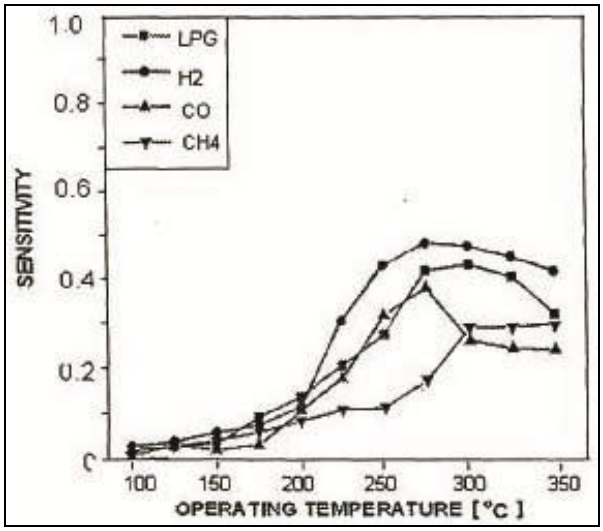

Fig 7: Sensitivity versus operating temperature for chemically prepared TiO_2 for different gases

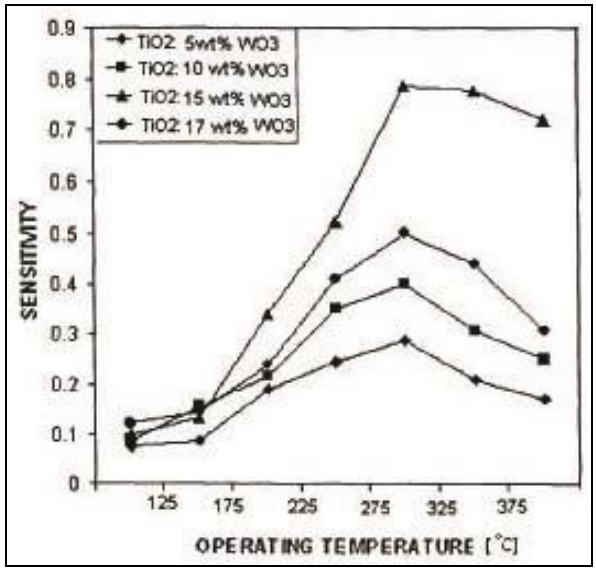

Fig 8: Sensitivity TiO_2 doped with different wt% of $WO_3$for H_2 gas

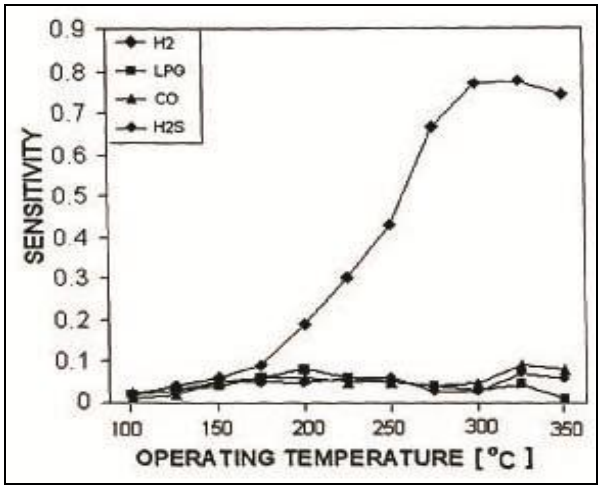

Fig 9: Sensitivity versus operating temperature for TiO_2.15 wt% WO_3 upon different gases exposure

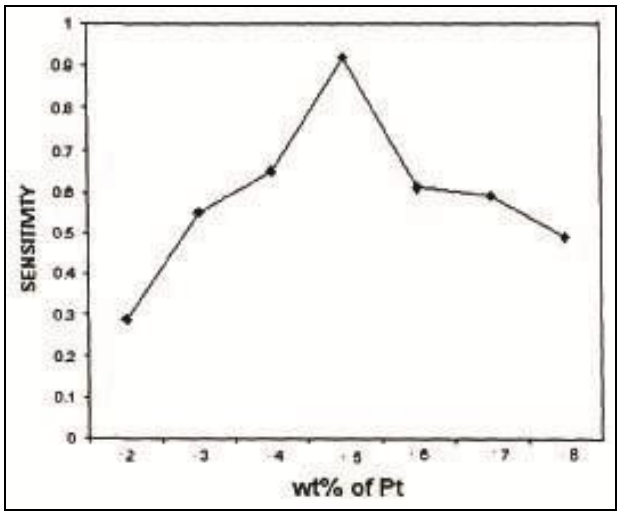

Fig 10: Sensitivity versus different wt % of Pt of 15 wt% WO_3 doped: TiO_2, H_2 Gas sensor

surpasses the conductance decrease caused by adsorbed oxygen, so that the resistance drops until 175ºC, where adsorbed oxygen or O^- acquires enough energy to transform into O" or O^{2}" making the resistance begin to increase slowly and reach a maximum at 300°C. When T > 300°C, the intrinsic conductance becomes dominant again due to enhanced thermal electronic activation and also due to desorption of oxygen adsorbates, so that resistance decreases with an increase in temperature. Compared with WO_3-doped TiO_2, the resistance of undoped TiO_2 decreased sharply with temperature. This indicates that the WO_3- doped TiO_2 can adsorb more oxygen than TiO_2 and that the effect of chemisorbed oxygen on the conductance is more remarkable for the WO_3-doped TiO_2. It was also observed that the amount of chemisorbed oxygen was larger for 15-wt% WO_3 -doped TiO_2 than those for 5, 10 and 20wt% WO_3 - TiO_2. It is obvious that the sensitivity is greatly dependent on the amount of chemisorbed oxygen. When the concentration of H_2 gas in air is the same, it is obvious that obtained highest sensitivity at an operating temperature 200°C, owing to the amount of

chemisorbed oxygen ions reaching the maximum at that temperature. Also, the sensitivities become improved with increasing the WO_3 content. It is reasonable to consider that the electrons introduced by substitution of more W^{6+} ions for the Ti^{4+} site of the TiO_2 lattice can form more chemisorbed oxygen ions on the surface. Moreover, it is worth noting that adding more WO_3, which facilitates the oxygen adsorption, significantly reduces the grain size of TiO_2.

Effect of Pt. Loading on Gas Sensitivity of 15 Wt%Wo_3 Doped Tio_2

The further improvement in gas-sensing properties was observed by addition of a small amount of noble metal. The maximum sensitivity for TiO_2: WO_3 : Pt sensor elements was found to be extraordinarily large, indicating that the H_2 detection was quite effectively sensitized by the addition of Pt. Fig. 11 shows the sensitivity of TiO_2: 15 wt% WO_3 : 0.5wt % Pt to 5000 ppm H_2 in air. The sensitivity for H_2 was observed to be 0.91 and 0.94 at an operating temperature 200°C and 225°C respectively. It was quite notable that the sensitivity increased with the Pt loading. The platinum concentration was varied from 0.2 to 1wt%. It was found that 0.5 wt% Pt was the optimum for the maximum sensitivity to H_2 gas at an operating temperature 200°C. Fig. 10 shows the increase in sensitivity when the Pt concentration was increased from 0.2 to 0.5wt% and then the decrease in sensitivity above 0.5 wt% Pt suggests the importance of dispersion of platinum on the semiconductor material.

Fig. 12 shows the sensitivity verses H_2 concentration in air (ppm) for TiO_2: doped 15 wt % WO_3:0.5 wt% Pt at an operating temperature 200°C. As seen from it, the sensitivity initially increased slowly with increasing the concentration and then linearly as the gas concentration increased from 600 to 1000 ppm. It is seen that the TiO_2:15 wt % WO_3:0.5 wt% Pt reaches the saturation value of sensitivity for concentration of 1000 ppm. The sensor is able to detect up to 200 ppm for H_2 with reasonable sensitivity at an operating temperature 200°C.

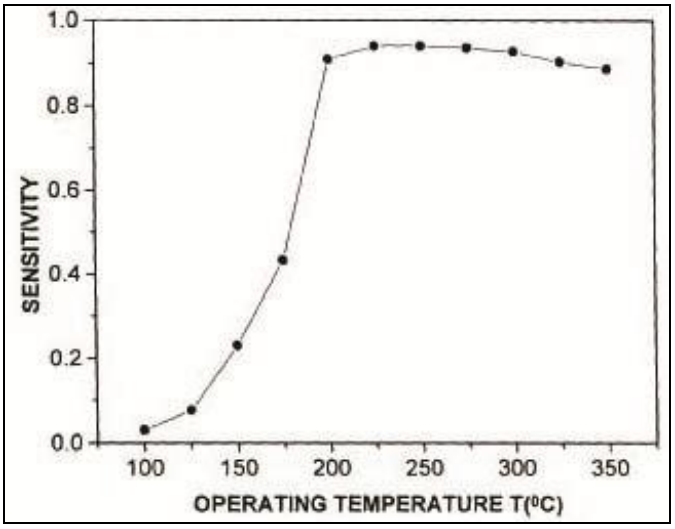

Fig 11: Sensitivity versus operating temperature for TiO_2:15 wt% WO_3 0.5 wt% Pt in presence of 5000 ppm of H_2 in air.

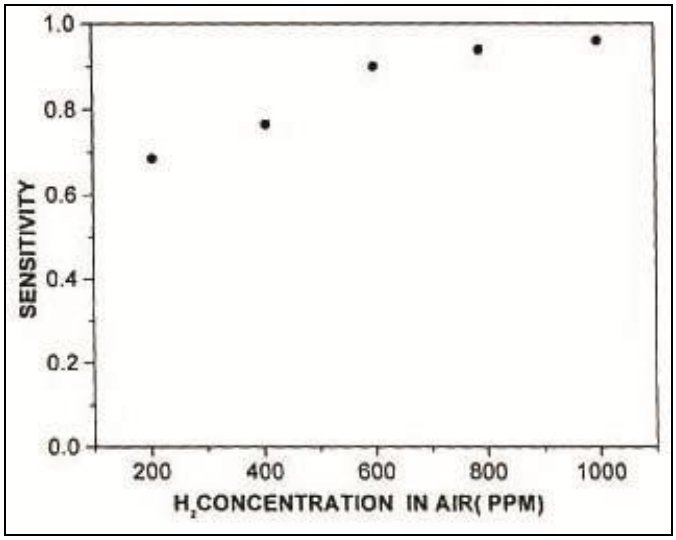

Fig 12: Sensitivity of TiO_2:15 wt% WO_3:0.5 wt % Pt for various concentration of H_2 in ppm leve

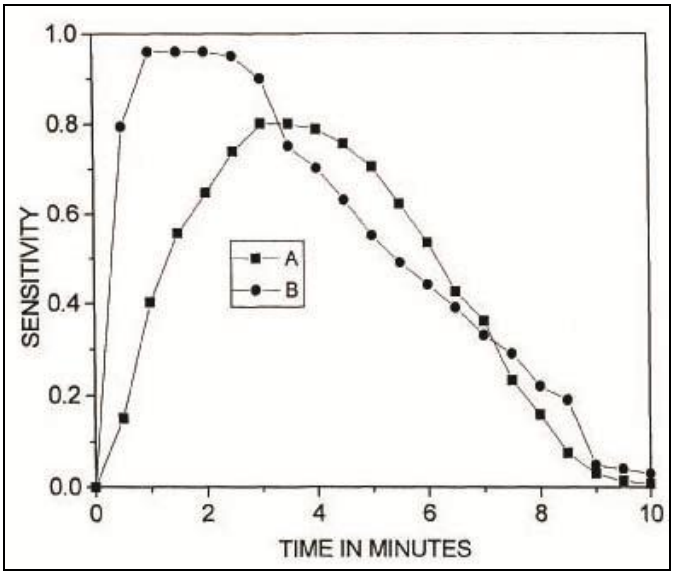

Fig 13: Response characteristics to 1000 ppm H2 (A) TiO_2:15% WO_3 and (B) TiO_2:15 wt% WO_3:0.5 wt% P

Fig. 13 shows a typical response characteristic of the sensor to 1000 ppm H_2 in air at an operating temperature 200°C. The response time is an important parameter to characterize a sensor. The response time is defined as the time taken to reach 90% of the response when gas of interest is introduced. Fig. 13 clearly shows that the response is fast with TiO_2: 15wt% WO_3:0.5wt% Pt, as compared with TiO_2:15wt% WO_3. The effect of Pt was thus seen not only in increasing the sensitivity to H_2 considerably but also the rate of response. This kind of sensitization has been well explained by an electronic interaction between the noble metal and the semiconductor oxide [31].

Conclusions

In conclusion, TiO_2 -based sensor doped with WO_3 and Pt

exhibited excellent H_2 -sensing properties with high sensitivity and response rates. XRD of TiO_2 calcined at 600°C for 6 h showed good crystalline quality with a grain size 54 nm. With its sensitivity superior to other oxides reported so far, the TiO_2-based sensor seems to be very promising as a semiconductor gas sensor especially for H_2 detection. The TiO_2: 15wt% WO_3 sensor doped with 0.5wt% Pt showed maximum sensitivity and selectivity to H_2 at an operating temperature 200°C.

References

1. Yamazoe N, Sens. Actuators B, 1991; 5:7-19.
2. Zakrzewska K, Thin Solid Films. 2001; 391:229-238.
3. Francioso L, Presicce DS, Taurino AM, Rella R, Siciliano P, Ficarella A, Sens. Actuators B, 2003; 95:66-72
4. Zakrzewska K, Vacuum. 2004; 74:335-338
5. Wang L, Pan L, Sun J, Hong YR, Kale GM, Mater J. Sci. 2005; 40:1717-1723
6. Mather GC, Marques FMB, Frade JR, European J. Cer. Soc, 1999; 19:887-891
7. Takami T. Ceram. Bull, 1988; 67:1956-1960.
8. Yamazoe N, Kurokawa Y, Seiyama T. Sens. Actuators B, 1983; 4:283-292.
9. Martinelli G, Carotta MC, Traversa E, Ghiotti G, MRS Bull, 1999; 24:30-36.
10. Guidi V, Butturi MA, Carotta MC, Cavicchi B, Ferroni M, Malagu C, Martinelli G, Vincenzi D, Sacerdoti M, Zen M, Sens, Actuators B, 2002; 84:72-77.
11. Sarala Devi G, Hyodo T, Shimizu Y, Egashira M, Sens. Actuators B, 2002; 87:122-129.
12. Sberveglieri G, Comini E, Faglia G, Atashbar MZ, Wlodarski W, Sens. Actuators B, 2001; 66:139-141
13. Yamazoe N, Miura N, in: Yamauchi S, Kodansha (Eds.), Technology, 4, Elsevier, Amsterdam, 19. 1992.
14. Takeuchi T, Oxygen sensors, Sens. Actuators 1988; 14:109-124.
15. Shimizu Y, Nakamura Y, Egashira M, Sens. Actuators B 1993; 13/14:128-131.
16. Tang H, Prasad K, Sanjines R, Levy F, Sens, Actu. B, 1995; 26/27:71.
17. Bange K, Ottermann CR, Anderson O, Jeschkowsky U, Laube M, Feile R, Thin Solid Films 1991; 197:279.
18. O'Regan B, Gratzel M. Nature 1991; 353:737.
19. Marguetettaz X, Fitzmaurice DJ. Am. Chem. Soc. 1994; 116:5017.
20. Huang SY, Kavan L, Exnar I, Gratzel MJ. Electrochem. Soc. 1995; 142:L142.
21. Sunada K, Kikuchi Y, Hashimoto K, Fujishima A. Sci. Technol. 1998; 32:726.
22. Liu X, Yang J, Wang L, Yang X, Lu L, Wang X, Mater. Sci. Eng. A, 2000; 289:241-245.
23. Atashbar MZ, Sun HT, Gong B, Wlodarki W, Lurb R. XPS Thin Solid Film 1998; 326:238.
24. Windiscmann H, Mark PJ. Electrochem. Soc. 1979; 126:627±633.
25. Birkefeld LD, Azad AM, Akbar SAJ. Am. Ceram. Soc, 1992; 75:2964-2968.
26. Tien TY, Stadler HL, Gibbons EF, Zacmana-dis PJ. Am. Ceram. Soc. Bull 1975; 54:280-285.
27. Logothesis EMJ. Solid State Chem. 1975; 12:331.
28. Azad AM, Akbar S, Younkman L. The Electrochemical Society Interface, 1994; 3(4):31-34.
29. Akbar SA, Younkman LB, EIectrochem J. Soc. 1997; 144:1750-1753.
30. Klug HP, Alexande LE. Wiley, New York, 1974; 125.
31. Vlachos DS, Papadopouls CA, Avaritsiotis JN. Sens. And Actuators B, 1997; 44:459-461